

Noise and Contraction Detection using Fetal Heart Rate and Accelerometer Signals During Labour

Jarle Urdal¹, Kjersti Engan¹, Trygve Eftestøl¹, Ladislaus Blacy Yarrot²,
Hussein Kidanto³ and Hege Ersdal^{4,5}

¹Dep. of Electrical Engineering and Computer Science, University of Stavanger, Norway,
 {jarle.urdal,kjersti.engan}@uis.no

²Research Institute, Haydom Lutheran Hospital, Tanzania

³School of Medicine, Aga Khan University, Tanzania

⁴Dep. of Anesthesiology and Intensive Care, Stavanger University Hospital, Norway

⁵Dep. of Health Sciences, University of Stavanger, Norway

Abstract

Fresh stillbirths and early neonatal deaths due to birth asphyxia are global challenges with an estimated 1.3 and 1.0 million deaths respectively every year. Adequate fetal monitoring during labour to prevent these deaths, is challenging, and regular assessment of fetal heart rate (FHR) in relation to uterine contractions is a key factor. A multi-crystal strap-on low-cost Doppler device, including an accelerometer, is recently developed to improve FHR monitoring in lower resource settings. In this work, we propose a method to increase interpretability of FHR Doppler signals by reducing noise, and a method to utilize accelerometer signals to estimate uterine contractions.

Keywords

Fetal Heart Rate, Doppler, Uterine contractions, Noise, Accelerometer

1 INTRODUCTION

Fetal heart rate (FHR) monitoring is a widely used method to assess the status of a fetus during pregnancy and labour. In high resource countries, cardiotocography (CTG) is normally used for all labours assessed as high risk. This measuring technique normally includes an external Doppler based FHR sensor and a tocometer to measure uterine contractions. In cases where the Doppler based sensor is insufficient in obtaining a good quality measurement, an alternative FHR sensor can be attached directly to the scalp of the fetus. In low resource settings, however, assessment of the FHR is often conducted manually using either a fetoscope or intermittent Doppler. As these techniques does not include information of the uterine contractions, the FHR is often not assessed in relation to the contractions.

Fresh stillbirths and asphyxia-related newborn deaths, meaning the fetus dies during labour or soon after birth, are global challenges with an estimated 1.3 and 1.0 million deaths respectively every year [1]. The vast majority of these, 98%, occurs in low resource settings [1], and the primary cause of these deaths is interruption of placental blood flow with ensuing changes in FHR patterns [1] [2] [3]. Optimal FHR monitoring should detect such changes at an early stage to facilitate adequate obstetric interventions.

The introduction of a portable, low-cost, multi-crystal Doppler continuous FHR monitoring device (Moyo, Laerdal Global Health, Stavanger, Norway) at several sites in Tanzania, provides the opportunity to study the FHR

changes and patterns without relying on human interventions to conduct periodic measurements. Well-known problems with such continuous Doppler devices are both noise and missing signal data. This can be caused by sensor movement, suboptimal placement of the sensor, maternal heart rate, doubling and halving of the FHR signal caused by the Doppler principle. Missing data can be estimated to resemble the measured data using dictionary learning [4] [5]. Artefacts due to noise may affect the interpretability and should be removed for both visual interpretation and further digital analysis. Methods for classification and suppression of this noise [6] and removal of the maternal heart rate [7] have previously been used on electrocardiography (ECG) signals from CTG. A system utilizing the sampled heart rate is, however, desired for low-cost continuous FHR monitoring devices for increased visual interpretation of the FHR.

Interpretation of the FHR signal during labour is normally conducted in relation to the corresponding uterine contraction, if this measurement is available. Accelerometers have previously been used to monitor muscle contractions [8], and muscular fatigue [9]. Signals from an accelerometer attached to the abdomen during labour has been shown to correlate to uterine contractions [10]. By utilizing an accelerometer mounted in close proximity of the Doppler sensor, indications of when contractions occur can potentially be extracted. In this work, we have studied Doppler and accelerometer signals from Moyo and identified time periods in the measured FHR where the signal is likely to be noise. Using the three-



Figure 1 The Laerdal Moyo fetal heart rate monitor. Reprinted with permission [13].

axes accelerometer, we indicate the position where uterine contractions occur.

2 DATA MATERIAL

The data is collected as part of the Safer Births research project, which is a research collaboration between multiple international research institutions, and hospitals in Tanzania. Data is collected at two urban and one rural hospital in Tanzanian between October 2015 and June 2018. In total, 3807 labours were recorded. Of these, 3593 were classified as normal 24 hours after birth, 184 were still admitted to a neonatal care unit, 18 died during the first 24 hours, and 12 died during labour. Only labours which were assessed as normal on admission to the hospital were included in the study.

Data collection was done using the Laerdal Moyo fetal heart rate monitor [11], illustrated in Figure 1. The device consists of a main unit with a display presenting the measured heart rate to the health care personnel, and a sensor unit with a Doppler ultrasound sensor and an accelerometer. The sensor unit is attached to the mother using an elastic strap. If the detected FHR stays outside the 110-160 range for 10 minutes, or outside the 100-180 range for 3 minutes, an alarm will sound to alert the health care personnel. The FHR is measured using a 9-crystal pulsed wave Doppler ultrasound sensor operating at a frequency of 1MHz and an intensity of less than 5mW/cm². The FHR is computed from the Doppler signal twice per second, i.e.

equivalent to sampling rate 2Hz. This gives a discrete FHR signal $fhr(n)$, where $n \in \mathbb{N}$ refers to the discrete index. Movement of the sensor unit is measured using a three-axes accelerometer, sampled at 50Hz. This gives the discrete acceleration signals $Acc_x(m)$, $Acc_y(m)$ and $Acc_z(m)$ at the x, y, and z directions respectively, where $m \in \mathbb{N}$ refers to the discrete index.

The project was ethically approved prior to implementation by the National Institute for Medical Research (NIMR) in Tanzania (NIMR/HQ/R.8a/Vol. IX/1434) and the Regional Committee for Medical and Health Research Ethics (REK) in Norway (2013/110/REK vest).

3 METHOD

This section first introduces a method to identify regions in the FHR measurement where the heart rate is less trustworthy, and thus should be removed. A proposed method of estimating the point in time when contractions occur based on acceleration signal follows. An example of the recorded signals is shown in Figure 2. The upper plot shows the FHR signal, and the lower plot shows the corresponding accelerometer. In the following we will use the notation $\dot{x}(n)$ to denote the discrete derivative of the signal $x(n)$.

3.1 Noise detection

Noise introduced in the measured FHR, $fhr(n)$, can affect the visual interpretation conducted by medical personnel as well as introduce undesired artefacts in a continuous digital analysis. To identify time periods, hereafter called segments, where variations in the FHR cannot be explained from a physiological perspective, we first fill missing data in the FHR using forward replication, given by

$$fhr_{rep}(n+1) = fhr(n); fhr(n+1) = 0 \quad \forall n \quad (1)$$

Let s be a pair of indexes (t_s, k) representing the start point and length of a segment. Let A be a set of s ,

$$A = \{s: |f\dot{h}r_{rep}(t_s)| > c \cap |f\dot{h}r_{rep}(t_s + k)| > c \cap k < T_K\} \quad (2)$$

Where T_K is the maximum allowed segment length, and c a threshold for the change in heart rate. As the measured FHR is a result of a biological process, physiological limitations exist for how fast the heart rate can change, the threshold c is set to 30 beats per minute. The segments are thereafter checked in order from the shortest to the largest, to see if the large signal variation is a doubling or halving caused by a Doppler shift error. Let $fhr_d(n)$ and $fhr_h(n)$ denote the intersample variation, and be defined by:

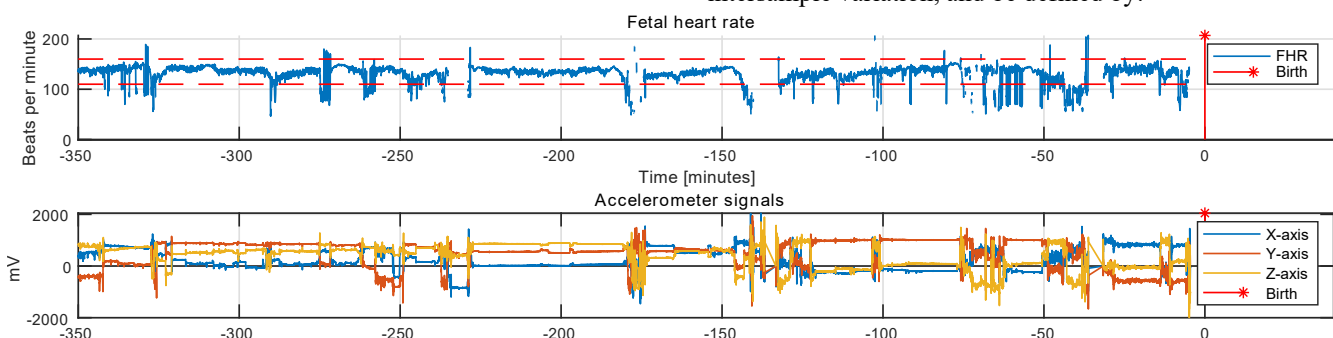


Figure 2 Signal example recorded using the Moyo fetal heart rate monitor. The red dashed lines indicate the normal region of the fetal heart rate. In the bottom plot, the three acceleration axes can be observed.

$$fhr_h(n) = |2 \cdot fhr(n) - fhr(n-1)| \quad (3)$$

$$fhr_d(n) = |0.5 \cdot fhr(n) - fhr(n-1)| \quad (4)$$

The shift errors are identified by comparing the intersample variation to a threshold T_D , allowing for some intersample variability. The shift errors are corrected using:

$$fhr_c(n) = 2 \cdot fhr(n) : fhr_h(n) < T_D \quad (5)$$

$$fhr_c(n) = .5 \cdot fhr(n) : fhr_d(n) < T_D \quad (6)$$

T_D is set to 5 based on empirical observation. If the sharp variations do not correspond to doubling or halving, the segment is considered as noise. When all segments of length $< T_K$ are checked, the process is repeated using backward replication as some segments may be $> T_K$ due to replication of missing data in the end of the segment. Based on findings from our previous work [5], the threshold T_K is set to 50 samples, equivalent to 25 seconds. A cleaned FHR signal is returned. An overview of the method is shown in Algorithm 1.

Algorithm 1 noisedetect

Input: fetal heart rate, fhr

Variation threshold, c

Maximum length of segment, T_K

Doubling/halving variation threshold, T_D

Output: cleaned fetal heart rate, fhr_c

$fhr_c = fhr$

for direction \in {forward, backward}

$fhr_{rep}(n) = \text{fillGaps}(fhr_c(n), \text{direction})$

$A = \{s : |fhr_{rep}(t_s)| > c \cap$

$|fhr_{rep}(t_s + k)| > c \cap k < T_K\}$

for all $s \in A$ sorted from smallest k

for all $i \in \{t_s, t_s + k\}$

$fhr_c(i) = 2 \cdot fhr(i) : fhr_h(n) < T_D$

$fhr_c(i) = .5 \cdot fhr(i) : fhr_d(n) < T_D$

$fhr_c(i) = 0 : |fhr(i)| > T_D$

$fhr_{rep}(n) = \text{fillGaps}(fhr_c(n), \text{direction})$

end while

end for

procedure $fhr_{rep} = \text{fillGaps}(fhr_{rep}, \text{direction})$

if direction = forward

$fhr_{rep}(n+1) = fhr_{rep}(n) : fhr_{rep}(n+1) = 0 \forall n$

else

$fhr_{rep}(n-1) = fhr_{rep}(n) : fhr_{rep}(n-1) = 0 \forall n$

end procedure

3.2 Estimation of contractions

An advantage of indicating the positions of the uterine contractions based only on the acceleration signal, allows the algorithm to run on recordings independent of missing FHR. The accelerometer captures small movements in the abdomen muscle as well as larger movements due to the

mother changing positions. The acceleration signal amplitude of these movements is, however, typically vastly different. As the sensor location and orientation may be different between each labour, a trend describing the movement is computed using the acceleration energy, $Acc_E(n)$, given by:

$$Acc_E(m) = \sqrt{Acc_x^2(m) + Acc_y^2(m) + Acc_z^2(m)} \quad (7)$$

As the acceleration energy signal contains high frequency components, an upper envelope is computed to obtain the movement trend. The envelope of the acceleration energy, $Acc_{env}(m)$, is computed using a 20 second window. A set of positions, C , indicating contractions at time points, t_c , are found as local peaks of the envelope, given by

$$C = \{t_c : \dot{Acc}_{env}(t_c) = 0 \cap T_1 < Acc_{env}(t_c) < T_2\} \quad (8)$$

Where the thresholds T_1 and T_2 are set to 10^{-2} and 10^{-1} standard gravity, g_0 , correspondingly, to avoid detecting small movements, and movements due to the mother changing position as contractions. As the intrapartum fetal monitoring guidelines from the International Federation of Gynecology and Obstetrics (FIGO) [12] states that <5 per 10-minute window averaged over 30 minutes is considered normal, the onset of two consecutive indicated contractions must occur at least 2 minutes from each other. The indicated contractions are hereafter called detected contractions. A pseudocode of the proposed contraction detection is depicted in Algorithm 2.

Algorithm 2 contractions

Input: Acceleration signals, Acc_x, Acc_y, Acc_z

Output: Set positions for detected contractions, C

$$Acc_E(m) = \sqrt{Acc_x^2(m) + Acc_y^2(m) + Acc_z^2(m)}$$

$$Acc_{env}(m) = \text{envelope}(Acc_E(m))$$

$$C = \{t_c : \dot{Acc}_{env}(t_c) = 0 \cap T_1 < Acc_{env}(t_c) < T_2\}$$

4 EXPERIMENTS AND RESULTS

As the dataset does not include measurements or registrations describing when uterine contractions or noise on the FHR signal occurs, experiments were devised to utilize both visual interpretation and statistics from the complete dataset to assess if the results from the proposed algorithms are reasonable. Experiments with visual interpretation of detected contractions on signals with low, medium, and high amounts of energy in the acceleration signal were chosen. The visual interpretation is based on discussions with trained midwives and the FIGO guidelines[12].

4.1 Noise removal

An example illustrating an example FHR signal, and the corresponding signal after noise removal is removed is shown in Figure 3. The method successfully identifies many of the outliers as noise, while some segments in the 75bpm region is kept. At the first stage of the data collection, the first generation Moyo was used. At a later stage, a second generation Moyo was used, and the percentage of missing data as well as noise was decreased.

The algorithm was run on the complete dataset. An overview of the amount of detected noise is shown in table 1.

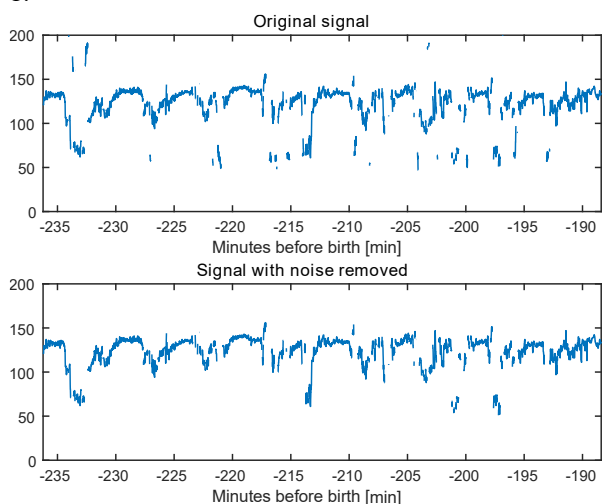


Figure 3 Example of noise detection and removal. Original signal on top, with some artefacts. Filtered signal on the bottom.

Number of episodes	3807
Total duration of all episodes	14201 hours
Percentage of all samples with detected, and corrected, Doppler shift error	0.22
Percentage of all samples removed	2.73

Table 1 Overview of the detected noise in the complete dataset.

4.2 Contractions on signals with low energy in the acceleration signal

Detection of contractions were conducted on a recording with low amount of energy in the acceleration signal extracted from the dataset, Figure 4. The FHR signal shows decelerations, which typically occur as a fetal response to a contraction. In the Figure we show the time points of detected contractions using red markers. It is easily seen that contractions corresponding to the 6 largest decelerations are detected. The contraction associated to the deceleration with a smaller drop in heart rate, at approximately 86 minutes before birth, is not considered to be caused by a contraction as it is too close to the previous

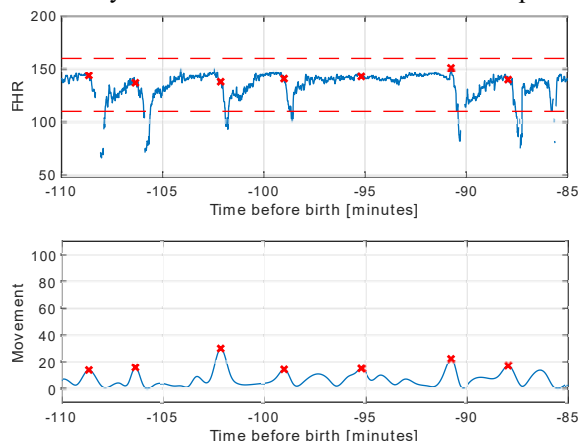


Figure 4 Detected contractions on a signal with low energy in the acceleration signal. The red dashed lines

indicate the normal range of the FHR. The red crosses indicate the detected contractions.

detected contraction. An additional uterine contraction is detected at approximately 95 minutes before birth, without a corresponding deceleration in the FHR.

4.3 Contractions on signals with medium energy in the acceleration signal.

Detection of contractions were conducted on a recording with medium amount of energy in the acceleration signal from the dataset, Figure 5. Contractions are detected periodically in the first half of the signal, while only one contraction are detected in the second half. Due to the quality of the FHR signal, it is challenging to assess if these are actual uterine contractions.

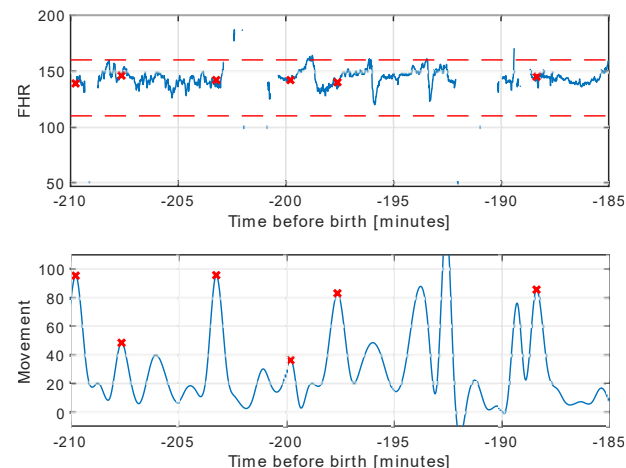


Figure 5 Detected contractions on a signal with a medium energy in the acceleration signal. The red dashed lines indicate the normal range of the FHR. The red crosses indicate the detected contractions.

4.4 Contractions on signals with high energy in the acceleration signal

Detection of contractions were conducted on a recording with high amount of energy in the acceleration signal from the dataset, Figure 6. Four uterine contractions are detected in the 25-minute window, but it is challenging to assess if these are actual contractions due to the FHR signal quality.

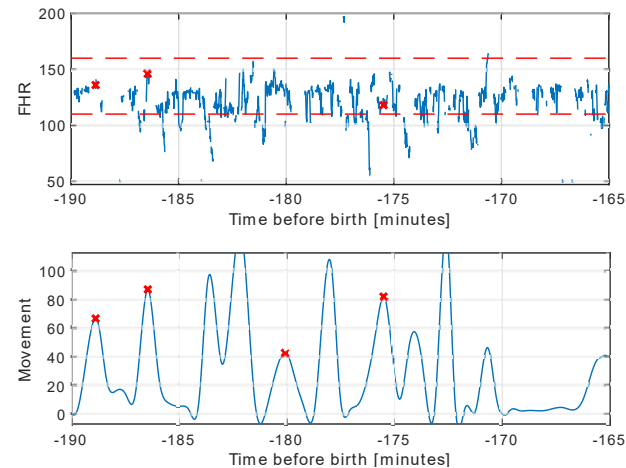


Figure 6 Detected contractions on a signal with a high energy in the acceleration signal. The red dashed lines

indicate the normal range of the FHR. The red crosses indicate the detected contractions.

4.5 Overview of contractions on complete dataset

The algorithm was run on all 3807 recordings in the dataset to indicate how many contractions were found, the mean time between contractions and other performance metrics. The results are shown in table 2.

Episodes with detected contractions	3753
Episodes without detected contractions	54
Median number of detected contractions per episode	29 [14, 51]
Median length of episode	171 [90, 304]
Mean time between contractions	6.27 minutes

Table 2 Overview of the detected uterine contractions in the complete dataset.

5 DISCUSSION

The noise-detection algorithm identifies many small sections of the FHR signal as noise. By removing these, a cleaner version of the FHR signal, and thereby the trend can be obtained. This may result in improved visual interpretation as well as it opens for automated signal analysis and feature extraction for future work. As it is difficult to determine with certainty which part of the measured FHR signal that is noise, only time periods where the signal is very unlikely to contain information of the fetal status is removed. This conservative approach results in that some periods containing noise may be kept.

Information of when uterine contractions occur can sometimes be found by studying the FHR signal itself, as the fetus might respond to a contraction by a deceleration. A challenge in this approach is that uterine contractions may cause increased movement of the mother and sensor, thus increasing the amount of missing data in the FHR.

The proposed method correctly identifies contraction waveforms corresponding to all six large decelerations in the example with low amount of movement, seen in Figure 4. These decelerations are confirmed by experienced midwives to resemble typical examples of decelerations caused by uterine contractions. The detected contraction at 95 minutes before birth may still be an actual uterine contraction, even if it does not have a deceleration in the measured FHR. The time periods in between the detected contractions resembles typical labour, and it would be less typical if there was not detected a contraction at the 95-minute point. When the energy in the acceleration signal increase, as seen in Figure 5, less contractions are detected. As the number of contractions during a 10-minute window varies from labour to labour, it is difficult to do a direct comparison between recordings. In cases with a high energy in the acceleration signal, Figure 6, the movement create peaks with a higher amplitude than contractions. While the highest peaks, categorized as movement and therefore excluded, is not detected as contractions it is challenging to categorize remaining peaks as contractions and not artefacts due to the movement. In cases where the FHR signal contains a large amount of missing data, the corresponding acceleration signal often contains more maternal movement. That is resulting in a lower identification of uterine contractions. In addition, real

contractions may in some cases occur at a higher rate than 5 per 10-minute windows, known as tachysystole. In the proposed algorithm, a threshold of minimum 2 minutes between the onset of two concurring uterine contractions is used, and this may be a limiting factor to detect tachysystole.

5.1 Limitations

A limitation of this work is the lack of tocometer measurements and manual annotations of the positions where uterine contractions occur in the dataset. To overcome this challenge, discussions regarding noise removal and indication of likely uterine contractions has been conducted during the study with trained health care personnel.

6 CONCLUSION

The work presented indicates that a large portion of the noise present in the FHR signal from Moyo can be removed utilizing only the sampled heart rate. It also indicates that a three-axes accelerometer mounted in proximity of the Doppler sensor, i.e. Moyo Fetal Heart Rate Monitor, can be used to estimate the point in time where contractions occur when the maternal movement is low. Further work validating indication positions of contractions with the use of a tocometer or manually annotated data must be conducted to determine the real performance.

7 ACKNOWLEDGEMENT

This work is part of the Safer Births project which has received funding from Laerdal Foundation, Laerdal Global Health, Skattefunn, Norwegian Ministry of Education and USAID. The work was partly supported by the Research Council of Norway through the Global Health and Vaccination Programme (GLOBVAC) project number 228203. Validation of the dataset has been conducted by Sara Brunner and Solveig Haukås Haaland at Laerdal Medical AS.

8 REFERENCES

- [1] Lawn, J.E., Blencowe, H., Waiswa, P., Amouzou, A., Mathers, C., Hogan, D., Flenady, V., Frøen, J.F., Qureshi, Z.U., Calderwood, C., et.al "Stillbirths: rates, risk factors, and acceleration towards 2030" in *The Lancet*, Vol 387.10018, 587-603.
- [2] Blencowe, H., Cousens, S., Jassir, F.B., Say, L., Chou, D., Mathers, C., Hogan, D., Shiekh, S., Qureshi, Z.U., You, D., et.al. "National, regional, and worldwide estimates of stillbirth rates in 2015, with trends from 2000: a systematic analysis." in *The Lancet Global Health* 4.2, e98-e108, 2016
- [3] Ersdal, H., Eilevstjønn, J., Linde, J.E., Yeconia, A., Mduma, E.R., Kidanto, H., Perlman, J., "Fresh Stillbirths and Severly Asphyxiated Neonates Represent a Common Hypoxic ischemic Pathway," *Int J Gynaecol Obstet*, pp. 171-180, 2018.
- [4] Oikonomou, V.P., Spilka, J., Stylios, C., Lhostka, L., "An adaptive method for the recovery of missing samples from FHR time series", *Proceedings of the 26th IEEE International*

Symposium on Computer-Based Medical Systems,
337-342, 2013

- [5] Barzideh, F., Urdal, J., Hussein, K., Engan, K., Skretting, K., Mdoe, P., Kamala, B., Brunner, S., "Estimation of Missing Data in Fetal Heart Rate Signals Using Shift-Invariant Dictionary", 2018 26th European Signal Processing Conference (EUSIPCO), 762-766, 2018.
- [6] Preethi, D., Valarmathi, R.S., "Classification and Suppression of Noises in Fetal Heart Rate Monitoring: A Survey", *Microelectronics, Electromagnetics and Telecommunications*, 607-615, 2019.
- [7] Vullings, R., Peters, C., Mischi, M., Oei, G., Bergmans, J., "Maternal ECG removal from non-invasive fetal ECG recordings", 2006 International Conference of the IEEE Engineering in Medicine and Biology Society, 1394-1397, 2006.
- [8] Watakabe, M., Mita, K., Akataki, K., Ito, K., "Reliability of the mechanomyogram detected with an accelerometer during voluntary contractions", in *Medical and Biological Engineering and Computing*, Vol 41.2, 198-202, 2003.
- [9] Tarata, M., Spaepen, A., Puers, R., "The accelerometer MMG measurement approach, in monitoring the muscular fatigue", in *Measurement Science Review*, Vol 1.1, 2001.
- [10] de Lau, H., Rabotti, C., Haazen, N., Oei, S.G., Mischi, M., "Towards improving uterine electrical activity modeling and electrohysterography: ultrasonic quantification of uterine movements during labor", in *Acta obstetrica et gynecologica Scandinavica*, Vol 92.11, 1323-1326, 2013.
- [11] Laerdal Global Health, "Moyo Fetal Heart Rate Monitor," Laerdal Global Health, [Online]. Available: <https://www.laerdal.com/laerdalglobalhealth/doc/2555/Moyo-Fetal-Heart-Rate-Monitor>. [Accessed 27 August 2019].
- [12] Ayres-de-Campos, D., Spong, C.Y., Chandrachan, E., FIGO Intrapartum Fetal Monitoring Expert Consensus Panel, "FIGO consensus guidelines on intrapartum fetal monitoring: Cardiotocography", in *International Journal of Gynecology & Obstetrics*, Vol. 131.1, 13-24, 2015.
- [13] Laerdal Medical, Moyo fetal heart rate monitor, user guide, 20-08388/00026151 REV E